# Sensor Fault Detection and Diagnosis Based on SOMNNs for Steady-State and Transient Operation

Yu Zhang, Chris Bingham, Michael Gallimore, Zhijing Yang and Jun Chen
School of Engineering
University of Lincoln
Lincoln, U.K.
{yzhang, cbingham, mgallimore, zyang, juchen}@lincoln.ac.uk

*Abstract*— **The paper presents a readily implementable approach for sensor fault detection, identification (SFD/I) and faulted sensor data reconstruction in complex systems based on self-organizing map neural networks (SOMNNs). Two operational regimes are considered, i.e. the steady operation and operation with transients. For steady operation, SOMNN based estimation error (EE) are used for SFD. EE contribution plots are employed for SFI. For operation with transients, SOMNN classification maps are used for SFD/I comparing with the 'fingerprint' maps. In addition, extension algorithm of SOMNNs is developed for faulted sensor data reconstruction. The validation of the proposed approach is demonstrated through experimental data during the commissioning of industrial gas turbines.**

***Keywords-sensor fault detection, sensor fault identification, estimation error, self-organizing map neural network.***

## I. INTRODUCTION

Sensor fault detection and identification (SFD/I) has attracted considerable recent attention from engineers and scientists due to the benefits of reducing down-time and loss of productivity, and increasing the confidence of safety, quality and reliability of the system.

With regard to previously reported techniques for SFD/I, principal component analysis (PCA) and artificial neural networks (ANNs) have been the most popular candidate solutions. PCA based squared prediction error (SPE) is well established and extensively applied for SFD in industrial processes and power control [1-8]. However, since SPE alone cannot directly identify the faulted sensor, additional algorithms are developed for SFI. For instance, a sensor validity index (SVI) has been considered and developed for SFI [1-5], and SPE-contribution plots have been presented as a supplement to SPE for diagnosing sensor faults [6,7]. For SFD/I, proposed ANN techniques are mainly based on multi-layer perceptron techniques (MLPNNs) and self-organizing map neural networks (SOMNNs). MLPNNs have been compared with support vector machines (SVMs) for fault detection in rotating machinery, with the conclusion that the ANN's performance was generally better than SVM in terms of 'training overhead' and robustness [9]. Furthermore, SOMNNs have been proposed for fault detection of induction machines [10], with a study in [11] indicating that SOMNNs generally provide good solutions and give better results than approaches based on MLPNNs or other radial basis function neural network (RBFNN) techniques.

The use of traditional approaches, such as SPE, are suitable when the sensed variables are within a similar range at all times, in which case, when a reading falls outside a predetermined group 'average range', it is considered an outlier. However, under operational conditions that are subject to transient, bias and drifting during normal operation (as a result of power or loading changes), the results from the traditional methods can lead to excessive false alarms being triggered. Here, for operation subject to transients, SOMNN based classification maps are applied for SFD/I on multiple sensor groups with different sensed variables, where SOMNNs arrange high-dimensional data automatically by their topological properties through the 'black-box' approach, and result in numerical classifications.

Finally, after identifying a faulted sensor, it is possible in some circumstances to reconstruct the measurements expected from that sensor and thereby facilitate improved unit availability. Data reconstruction can be achieved by extensions of the SOMNN-based approaches [12] for SFD/I. In this paper, SOMNN based approaches are applied for SFD/I and faulted sensor signal reconstruction in industrial gas turbine systems.

## II. SELF-ORGANIZING MAP NEURAL NETWORK

A SOMNN is a competitive learning network. An input data vector, $\boldsymbol{x} = [x_1, x_2, \ldots, x_I] \in \Re^{I\times 1}$, with $I$ variables (sensors), is associated with a reference vector, $\boldsymbol{r}_i \in \Re^{I\times 1}$, which is often randomly initiated to give each neuron a displacement vector in the input space. For each sample of $\boldsymbol{x}(t)$, $\boldsymbol{r}_w(t)$ constitutes 'the winner', by seeking the minimum distance between the input vector and the reference vector, and is calculated from:

$$\left\|\boldsymbol{x}(t) - \boldsymbol{r}_w(t)\right\| \le \left\|\boldsymbol{x}(t) - \boldsymbol{r}_i(t)\right\| \text{ for } \forall \text{ i}. \quad (1)$$

After obtaining a 'winner', the reference vectors are updated using:

$$\boldsymbol{r}_i(t+1) = \boldsymbol{r}_i(t) + n_{w,i}(t)\left(\boldsymbol{x}(t) - \boldsymbol{r}_i(t)\right), \quad (2)$$

where $n_{w,i}(t)$ is a neighborhood function, which is normally chosen as Gaussian. The reference vectors are adjusted to match the training signals, in a regression process over a finite number of steps, in order to achieve the final 'self-organizing maps'. [13]

978-1-4673-4703-7/13/$31.00 ©2013 IEEE

## III. SFD/I FOR STEADY OPERATION

To provide an illustrative focus to the study, a group of six burner tip temperature sensors on an industrial turbine system is studied. Fig. 1 shows example field data from an experimental trial showing a sensor fault on sensor 6. Here, data from the first 300 minutes are used as training data, and data from 300 to 1440 minutes are applied as testing data.

SOMNN is performed using these measurements, with 6 sensor variables and 1440 time samples in the network. To provide a numerical output of the results, an estimation error (EE) is introduced to monitor the performance of the final 'self-organizing maps':

$$EE = \left\| \boldsymbol{x}^{new} - \boldsymbol{r}_w^{new} \right\|, \tag{3}$$

which is defined as the distance between the winning weight vector $\boldsymbol{r}_w^{new}$ and the input vector $\boldsymbol{x}^{new}$ in the new state. If EE is greater than a pre-determined percentage of the normal distribution profile, the new state signal is considered to be abnormal, i.e. when

$$EE > \delta_2 . \tag{4}$$

Here, for example, here, the threshold is selected as the 99.7% confidence level from the training data. The EE plot is shown in Fig. 2(a) for the same experimental trial—the faults becoming evident after 500 minutes.

SFI is simply achieved from the contribution plots. The contribution to the EE from each sensor is calculated and plotted in percentage form, as shown in Fig. 2(b). A higher percentage represents a greater 'error contribution' from that sensor. The error contribution plot is used as a complement for the EE plot to accomplish the SFI after abnormal conditions have been initially detected. It is shown that sensor 6 is at fault after 500 minutes in this case.

The EE result in Fig. 2(a) is compared with the result from the traditional PCA based SPE on a same confidence level, as shown in Fig. 3. Although the error measure EE and the SPE are based on different algorithms, it can be seen that the detecting results from both methods are comparable and in good agreement.

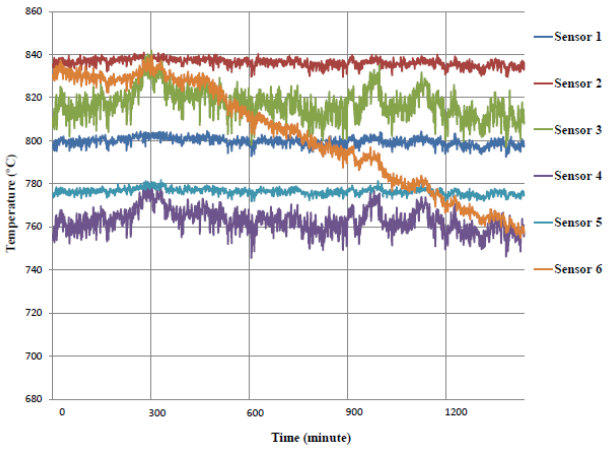


Figure 1. Experimental trial: temperature information

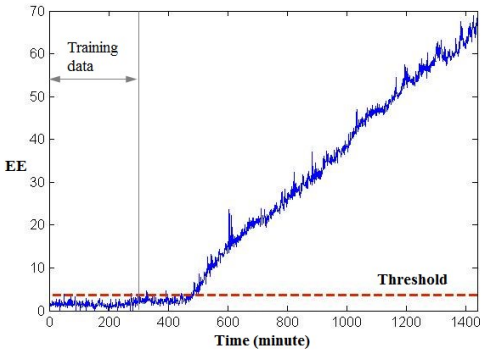


(a)

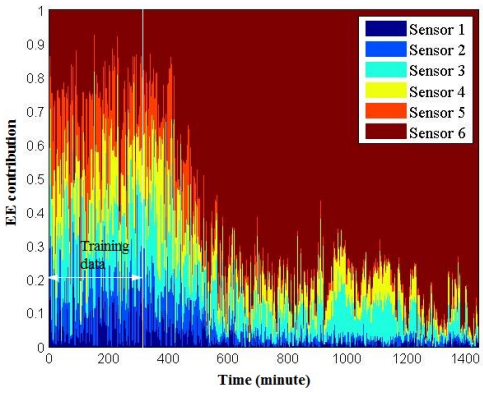


(b)

Figure 2. (a) EE; (b) EE contribution plot

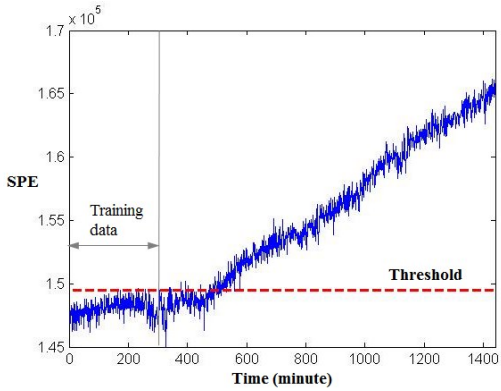


Figure 3. SPE for experimental trial

Although the SOMNN based EE techniques have been demonstrated to be applicable for real-time SFD/I on industrial systems, they can only be readily applied to operation in steady state, with the same disadvantage of PCA based SPE, and will lead to excessive false alarms when applied to notionally normal operation that is subject to significant transients caused by changes of loading and power, for instance. For use in such circumstances, therefore, SOMNN based classification maps are now introduced for SFD/I.

## IV. SFD/I FOR OPERATION WITH TRANSIENTS

The value of using SOMNN for SFD/I is demonstrated by use of example case studies. Here, a group of 16 sensors is

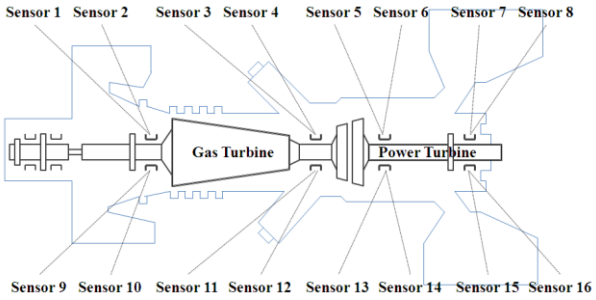


Figure 4. The location of the 16 sensors on a turbine system

considered, including 8× bearing vibration measurements (sensors 1 to 8) and 8× bearing temperature sensors (sensors 9 to 16), sited on a twin shaft (generator and power) industrial turbine unit, with X and Y sensor orientations on either end of each shaft, as shown in simplified form in Fig. 4.

The SOMNN training is performed initially using the measurements shown in Fig. 5, with 16 variables and 1440 time samples (daily data) in the network. To obtain a visual output of the classifications, initially, the SOMNN is trained with the output space as 8×8 hexagonal grids, using *Matlab Neural Network Toolbox* [14]. The weighting matrices in the component planes for the 16 sensors are shown in Fig. 6.

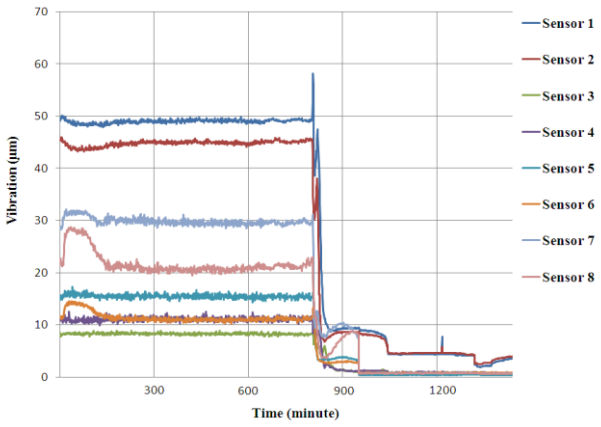


(a)

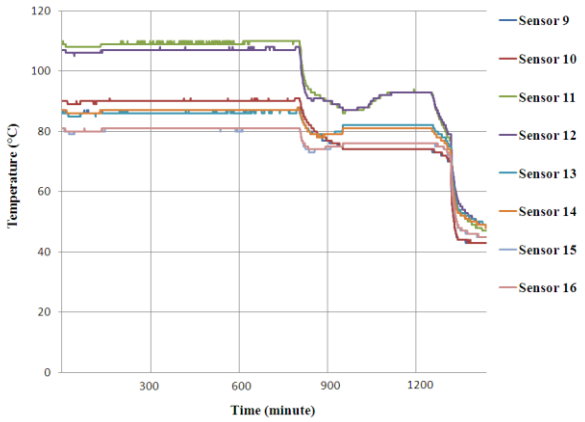


(b)

Figure 5. Normal operation with transients: (a) vibration information; (b) temperature information

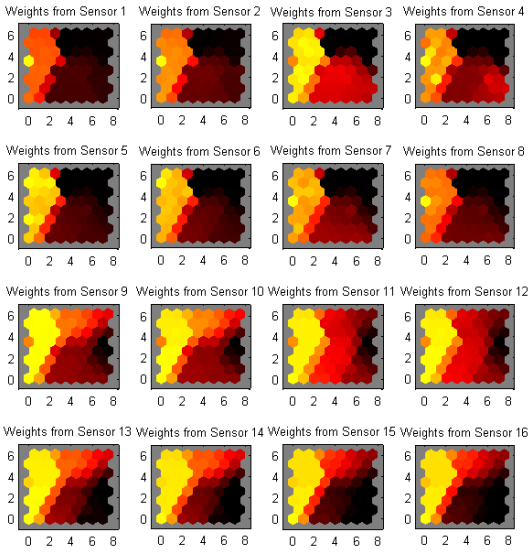


Figure 6. Component planes of the map for normal operation

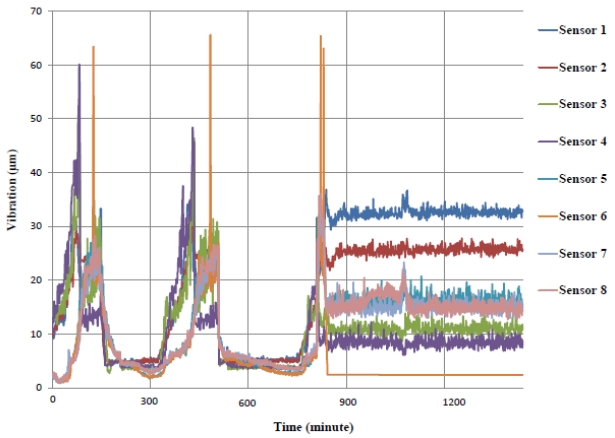


(a)

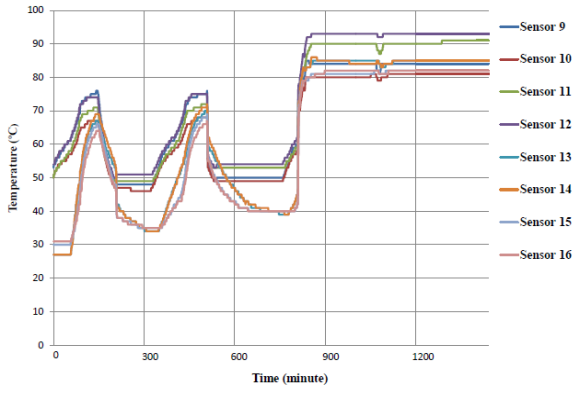


(b)

Figure 7. Operation with fault on sensor 6: (a) vibration information; (b) temperature information

TABLE I
CLASSIFICATION MAPS FOR NORMAL OPERATION

| Sensor Index | 1 | 2 | 3 | 4 | 5 | 6 | 7 | 8 | 9 | 10 | 11 | 12 | 13 | 14 | 15 | 16 |
|---|---|---|---|---|---|---|---|---|---|---|---|---|---|---|---|---|
| Classification Map I | 1 | 1 | 1 | 1 | 1 | 1 | 1 | 1 | 2 | 2 | 2 | 2 | 2 | 2 | 2 | 2 |
| Classification Map II | 2 | 2 | 2 | 2 | 2 | 2 | 2 | 2 | 1 | 1 | 1 | 1 | 1 | 1 | 1 | 1 |

TABLE II
CLASSIFICATION MAPS SHOWING FAULT ON SENSOR 6

| Sensor Index | 1 | 2 | 3 | 4 | 5 | 6 | 7 | 8 | 9 | 10 | 11 | 12 | 13 | 14 | 15 | 16 |
|---|---|---|---|---|---|---|---|---|---|---|---|---|---|---|---|---|
| Classification Map I | 1 | 1 | 1 | 1 | 1 | 2 | 1 | 1 | 1 | 1 | 1 | 1 | 1 | 1 | 1 | 1 |
| Classification Map II | 2 | 2 | 2 | 2 | 2 | 1 | 2 | 2 | 2 | 2 | 2 | 2 | 2 | 2 | 2 | 2 |
| Classification Map III | 1 | 1 | 1 | 1 | 1 | 2 | 1 | 1 | 2 | 2 | 2 | 2 | 2 | 2 | 2 | 2 |
| Classification Map IV | 2 | 2 | 2 | 2 | 2 | 1 | 2 | 2 | 1 | 1 | 1 | 1 | 1 | 1 | 1 | 1 |

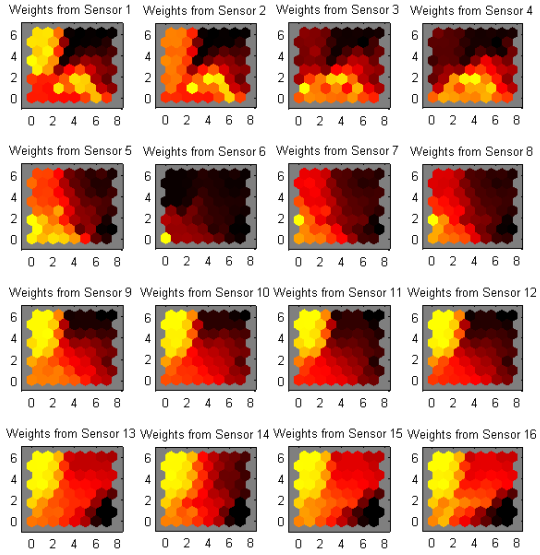


Figure 8. Component planes of the map showing fault on sensor 6

It is evident that there is a clear separation of the weighting matrices between sensors 1 to 8 and sensors 9 to 16 during normal operation. During operation that is considered to be 'abnormal' (depicted in Fig. 7), the component planes of the map are shown in Fig. 8, where the weighting matrix for sensor 6 is clearly different from those of the other sensors.

To provide the classifications numerically, the SOMNN is trained to classify the data from the 16 sensors into 2 patterns, i.e. instead of 64 neurons in the output layer, here, there are only 2 outputs (with indices 1 or 2). The classification maps for normal operation result in two forms (since there are no target classifications, output 1 or 2 could be chosen randomly for one pattern), as shown in Table I, which again shows a separation of the classifications between sensors 1 to 8 and sensors 9 to 16. Having been trained, the network is applied to data from the unit on a real-time basis to detect deviations from normal behaviour.

By way of example, the measurements of Fig. 7 are applied to the SOMNN and the 2-classification procedure applied. The results are shown in classification map I, of Table II, where sensor 6 is clearly identified as not being classified with the remaining sensors (matching the component planes in Fig. 8), and therefore indicates 'abnormal characteristics', as expected in this case. The possible types of classification maps that would show potential sensor faults on sensor 6 are given in the form of alternative 'classification maps II, III and IV'. Map II is just a variant of map I which again shows the sensor 6 is behaving differently from the remainder. Map III or IV also show that the sensor is not clustered in its normal group, again indicating a potential sensor fault.

An advantage of using SOMNNs is that they are simply realized with a basic numeric output. However, the 'black-box' nature of ANNs provides little insight into the relationship between the actual inputs, and the ultimate confidence in the final results at the output. Nevertheless, the SOMNN has been shown to be effective as a warning of sensor faults, and for discriminating which sensor is at fault.

## V. DATA RECONSTRUCTION

Following the identification of a faulted sensor, a decision needs to be made as to whether operation of the unit can continue, or whether the unit should be shut-down for immediate maintenance—the latter obviously leading to enforced down-time and lost productivity. An alternative, therefore, is to attempt to reconstruct a 'best estimate' of the measurements expected from the faulted sensor with a view to retaining the ability to keep the unit operating.

Based on SOMNN algorithm, for a 2-dimensional output space, the faulted signal can be reconstructed by adjusting the weight vector using a combination of its $k$ nearest nodes. Firstly, an activation function is defined to measure the

activation of output neuron $n$ for an input vector $\boldsymbol{x}$ by using a Gaussian kernel:

$$T(n) = \exp\left( \frac{-1}{2\sigma_n^2} \left\| \boldsymbol{x} - \boldsymbol{r}_n \right\|^2 \right), \tag{5}$$

where $\sigma_n^2$ is a parameter representing the influence region of neuron $n$. When the current sample of the sensor is detected as

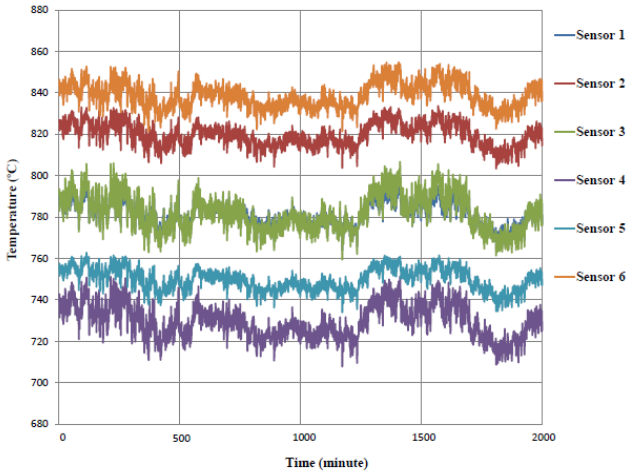


Figure 9. Data reconstruction test example

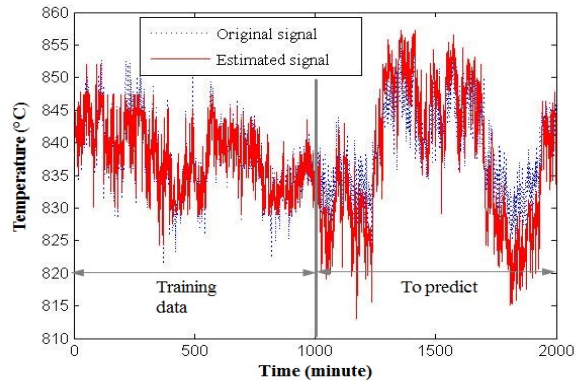


(a)

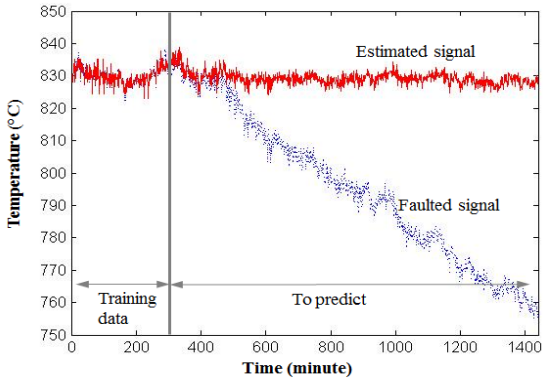


(b)

Figure 10. Data reconstruction based on SOMNN: (a) test example; (b) faulted signal

being faulty, the winning neuron for this measurement is no longer valid, and the weighting vector can be estimated by considering the $k$ nearest neighbouring neurons of the corresponding winning neuron in the output space, and expressed as

$$\boldsymbol{z}_i \approx \sum_{m=1}^{k} \left( T_m \boldsymbol{r}_{im} \right) \Big/ \sum_{m=1}^{k} T_m , \tag{6}$$

where $\boldsymbol{z}_i$ is the estimation of the measurement, $i$ is sensor index and $m$ is the neuron index.

To evaluate the reconstruction performance, define the $l_2$-norm relative reconstruction error, $E$, as follows

$$E = \frac{\sqrt{\sum_{i=1}^{I} || \boldsymbol{z}_i - \boldsymbol{x}_i ||_2^2}}{\sqrt{\sum_{i=1}^{I} || \boldsymbol{x}_i ||_2^2}} . \tag{7}$$

As a test example, normal operational measurements from the burner tip temperature sensors are studied, as shown in Fig. 9. The first 1000 minutes are used as training data, and signal for sensor 6 from 1000 to 2000 minutes is estimated. The original and estimation signals are shown in Fig. 10(a). The $l_2$-norm relative prediction error is 0.003% for the test example, signifying that the reconstruction bears an excellent correspondence with the 'real' measurements.

Then, the method is applied to the experimental trial with sensor failure as shown in Fig. 1. The faulted signal is reconstructed as shown in Fig. 10(b). From the results it can be seen that from the onset of the 'fault period', the reconstructed data follows the normal trend (given by the behaviour of the other sensors) very reliably, and could therefore be used in place of the erroneous measurements in the short term.

It should be noted that these techniques can also be readily adapted to provide expected outputs from each sensor in a group, which can then be compared to the real-time measurements, and thereby provide a further simple mechanism for detecting or corroborating unexpected characteristics.

## VI. Conclusion

In this paper, SOMNN based approaches are applied for SFD/I and faulted sensor data reconstruction, for steady and non-steady operations, separately. SOMNN based EE and contribution plots are particularly useful for real-time SFD/I during steady operation. For SFD/I during operation with transients, SOMNN is applied by comparing the classification map with the 'fingerprint' maps for normal operation. Moreover, data reconstruction is then performed using an extension of the proposed SOMNN technique. The proposed approaches are shown to be capable to detecting, identifying and reconstructing sensor faults successfully. The efficacy of the proposed approaches has been proved through the use of results from experimental trials.

## REFERENCES


[1] R. Dunia, S. J. Qin, T. F. Edgar, T. J. McAvoy. "Use of Principal Component Analysis for Sensor Fault Identification." *Computers Chem. Engng*, vol. 20, 1996, pp.713-718.

[2] H. H. Yue, S. J. Qin. "Reconstruction-based Fault Identification Using a Combined Index." *Ind. Eng. Chem. Res.*, vol. 40, 2001, pp.4403-4414.

[3] S. W. Choi, C. Lee, J. M. Lee, J. H. Park, I. B. Lee. "Fault detection and Identification of Nonlinear Processes Based on Kernal PCA." *Chemometrics and Intelligent Laboratory Systems*, vol. 75, 2005, pp.55-67.

[4] T. Xu, Q. Wang. "Application of MSPCA to Sensor Fault Diagnosis." *ACTA Automatica Sinica*, vol. 32, No.3, 2006, pp.417-421.

[5] B. Lee, X. Wang. "Fault Detection and Reconstruction for Micro-Satellite Power Subsystem Based on PCA." *Systems and Control in Aeronautics and Astronautics*, vol. 3, 2010, pp.1169-1173.

[6] S. Wang, F. Xiao. "Detection and diagnosis of AHU Sensor Faults Using Principal Component Analysis Method." *Energy Conversion and Management*, vol. 45, 2004, pp.2667-2686.

[7] H. Liu, M. J. Kim, O. Y. Kang, S. B, J. T. Kim, C. K. Yoo. "Sensor Validation for Monitoring Indoor Air Quality in a Subway Station." *Sustainable Healthy Buildings*, vol. 5, 2011, pp.477-489.

[8] J. Ni, C. Zhang, S. Yang. "An Adaptive Approach Based on KPCA and SVM for Real-time Fault Diagnosis of HVCBs." *IEEE Trans. on Power Delivery*, vol. 26, No.3, 2011, pp.1960-1971.

[9] L. B. Jack, A. K. Nandi. "Fault Detection Using Support Vector Machine and Artificial Neural Networks Augmented by Genetic Algorithms." *Mechanical Systems and Signal Processing*, vol. 16, No.2-3, 2002, pp. 373-390.

[10] S. Wu, T. W. S. Chow. "Induction Machine Fault Detection Using SOM-based RBF Neural Networks." *IEEE Trans. on Industrial Electronics*, vol. 51, No.1, 2004, pp. 183-194.

[11] K. Elissa, L. F. Gonçalves, J. L.Bosa, T. R. Balen, M. S. Lubaszewski, E. L. Schneider, and R. V. Henriques. "Fault Detection, Diagosis and Prediction in Electrical Valves using Self-organizing Maps." *Journal of Electron Test*, vol. 10, 2011, pp. 1007-1020.

[12] T. Kohonen, *Self-Organizing Maps*, Heidelberg: Springer Verlag, 1995.

[13] Fort, J.C., 2006, "SOM's mathematics," *Neural Networks*, vol. 19, pp. 812–816.

[14] *Matlab version 7.10.0*. Natick Massachusetts, the Mathworks Inc., 2010.